© 2015. Published by The Company of Biologists Ltd | Journal of Cell Science (2015) 128, 1542–1554 doi:10.1242/jcs.163295

RESEARCH ARTICLE

Synaptic control of mRNA translation by reversible assembly of XRN1 bodies

Luciana Luchelli[1,2,3], María Gabriela Thomas[1,2] and Graciela L. Boccaccio[1,2,3,*]

ABSTRACT

Repression of mRNA translation is linked to the formation of specific cytosolic foci such as stress granules and processing bodies, which store or degrade mRNAs. In neurons, synaptic activity regulates translation at the post-synapse and this is important for plasticity. N-methyl-D-aspartate (NMDA) receptor stimulation downregulates translation, and we speculate that this is linked to the formation of unknown mRNA-silencing foci. Here, we show that the 5′-3′ exoribonuclease XRN1 forms discrete clusters associated with the post-synapse that are different from processing bodies or stress granules, and we named them synaptic XRN1 bodies (SX-bodies). Using primary neurons, we found that the SX-bodies respond to synapse stimulation and that their formation correlates inversely with the local translation rate. SX-bodies increase in size and number upon NMDA stimulation, and metabotropic glutamate receptor activation provokes SX-body dissolution, along with increased translation. The response is specific and the previously described Smaug1 foci and FMRP granules show a different response. Finally, XRN1 knockdown impairs the translational repression triggered by NMDA. Collectively, these observations support a role for the SX-bodies in the reversible masking and silencing of mRNAs at the synapse.

KEY WORDS: P body, RNA granule, Stress granule, XRN1, Synapse

INTRODUCTION

Regulation of protein synthesis at the post-synapse contributes to synaptic plasticity. Different stimuli elicit mRNA-specific effects as well as global changes in translation. It was shown both in cultured neurons and isolated synaptoneurosomes that the activation of metabotropic glutamate receptors (mGluR) enhances global protein synthesis by multiple pathways. A different response follows N-methyl-D-aspartic acid receptor (NMDAR) stimulation, which globally attenuates protein synthesis at the synapse. Dendritic translation in cultured neurons expressing a GFP-based reporter is stimulated by exposure to dihydroxyphenylglycine (DHPG) – an agonist of mGluR – or NMDAR blockers, and incorporation of radioactive amino acids is reduced in neurons exposed to short pulses of NMDA (Marin et al., 1997; Job and Eberwine, 2001; Sutton et al., 2004). In addition, prolonged exposure of synaptoneurosomes to glutamate reduces amino acid incorporation; a 30-s exposure to glutamate plus NMDA provokes an acute reduction followed by an enhancement of protein synthesis at 15 minutes after the pulse. By contrast, continuous exposure to DHPG increases the incorporation of amino acids immediately after a pulse (Leski and Steward, 1996; Scheetz et al., 2000; Weiler et al., 2004). NMDAR stimulation affects translation through multiple mechanisms. It activates the mammalian/mechanistic target of rapamycin (mTOR), which in turn stimulates a number of translation factors and affects several miRNA targets in opposite directions (Weiler and Greenough, 1993; Banko et al., 2006; Sosanya et al., 2013). The integration of all these pathways results in the de-repression of a number of transcripts and the repression of others, and it was suggested that the reduction in the global protein synthesis rate induced by NMDA facilitates the translation of specific messengers, including that of Ca^{2+}/CaM-dependent protein kinase II (CaMKII) and activity-regulated cytoskeletal-associated protein (Arc, also known as Arg3.1) mRNAs, which appear to compete poorly with other transcripts (Marin et al., 1997; Scheetz et al., 2000; Sutton et al., 2004; Sutton et al., 2006; Sutton et al., 2007; Park et al., 2008).

In most cell types, translation inhibition is linked to the formation of supramolecular aggregates containing silenced messengers and associated repressors, which we have termed mRNA-silencing foci (Buchan and Parker, 2009; Thomas et al., 2011). Processing bodies are ubiquitous foci that contain several molecules involved in mRNA repression and decay. Historically, the mammalian 5′-3′ exoribonuclease 1 (XRN1) was the first RNA decay molecule detected in cytoplasmic foci (Bashkirov et al., 1997). Thereafter, the decapping factors DCP1 and DCP2 and additional decapping co-activators were reported to be present in the XRN1 foci (Ingelfinger et al., 2002). XRN1 is a conserved molecule that mediates the 5′-3′ degradation of 5′ monophosphate transcripts. XRN1 substrates are mostly decapped mRNAs and 3′ fragments produced by endonucleolytic cleavage during nonsense-mediated decay (NMD) or RNA-induced silencing complex (RISC)-mediated silencing (Lejeune et al., 2003; Gatfield and Izaurralde, 2004; Souret et al., 2004; Bagga et al., 2005; Jones et al., 2012; Nagarajan et al., 2013; Siwaszek et al., 2014). Remarkably, both in animals and plants, XRN1 deletion affects specific subsets of transcripts, suggesting that bulk mRNA decay is not the major activity of this enzyme (Souret et al., 2004; Rymarquis et al., 2011). Substrate specificity would be achieved through the preferential binding of XRN1, which might involve RNA binding proteins (RBPs) that could influence the recruitment of XRN1 to selected targets. For example, specific hexamer sequences at the 5′ end either stimulate or inhibit degradation by the plant homolog XRN4 through unknown mechanisms (Rymarquis et al., 2011). Moreover, recombinant mammalian XRN1 preferentially binds and degrades RNAs carrying G-quartets, which are important motifs for the binding of fragile X

[1]Fundación Instituto Leloir, C1405BWE Buenos Aires, Argentina. [2]Instituto de Investigaciones Bioquímicas Buenos Aires-Consejo Nacional de Investigaciones Científicas y Tecnológicas, C1405BWE Buenos Aires, Argentina. [3]Facultad de Ciencias Exactas y Naturales, University of Buenos Aires, C1428EHA Buenos Aires, Argentina.

*Author for correspondence (gboccaccio@leloir.org.ar)

Received 12 September 2014; Accepted 13 February 2015

Journal of Cell Science

Journal of Cell Science (2015) 128, 1542–1554 doi:10.1242/jcs.163295

mental retardation protein (FMRP) to dendritic transcripts (Bashkirov et al., 1997; Darnell et al., 2001). In addition, the expression of the *Drosophila* XRN1 homolog, termed Pacman, is controlled spatially and temporally, suggesting a regulatory role. Invertebrate XRN1 affects embryo development and fly pacman and *Caenorhabditis elegans* XRN1 control epithelial closure, wound healing and related morphological processes. Lower eukaryote XRN1 influences cell proliferation, and mutations in plant XNR4 affect the stress response and generate developmental abnormalities (Newbury and Woollard, 2004; Jones et al., 2013; Nagarajan et al., 2013). The biological relevance of vertebrate XRN1 is poorly described and, here, we show that rodent XRN1 responds to synaptic activity and regulates protein synthesis in hippocampal neurons.

NMDAR stimulation triggers translational silencing at the post-synapse, and we hypothesized that a specific type of processing body or related mRNA-silencing foci is concomitantly induced (Pascual et al., 2012). Different types of processing bodies containing subsets of components were reported in dendrites and synapse surroundings (Cougot et al., 2008; Zeitelhofer et al., 2008; di Penta et al., 2009; Miller et al., 2009; Pradhan et al., 2012). Here, we show that XRN1 forms clusters associated with the post-synapse that we termed synaptic XRN1 bodies (SX-bodies), as they do not contain the canonical processing body components DCP1A, Ge-1 (also known as Hedls, RCD8 or EDC4) or Rck (also known as p54 or DDX6) and are also different from the previously described Smaug1 (also known as Samd4a) foci (S-foci) and FMRP or survival of motor neuron (SMN1) granules. The XRN-1-positive bodies are also different from stress granules, which are specifically formed during the stress response. We found that the presence of XRN-1-positive puncta at the synapses of cultured hippocampal neurons is affected by synaptic stimulation and inversely correlates with the local protein synthesis rate. NMDAR stimulation enhanced SX-body formation and inhibited translation at spines and dendrites, whereas mGluR activation provoked the dissolution of the SX-bodies and stimulated local translation. We compared the behavior of the SX-bodies to that of S-foci and FMRP-positive granules, also involved in translational regulation at the synapse (Antar et al., 2004; Baez et al., 2011; Darnell et al., 2011; Graber et al., 2013). Similar to the SX-bodies, the S-foci and the FMRP-positive granules transiently dissolved upon DHPG, although with different kinetics. In striking contrast to the enhanced formation of the SX-bodies upon NMDAR stimulation, the S-foci dissolved and the FMRP-positive granules did not respond to NMDA, as reported previously (Antar et al., 2004; Baez et al., 2011). The size and number of XRN-1-positive bodies were affected by drugs that stabilize polysomes, suggesting that transcripts released from polysomes upon NMDAR stimulation are directed to the XRN1 bodies. Finally, the small interfering (si)RNA-mediated knockdown of XRN1 impaired the decrease in translation induced by NMDA. Collectively, these observations suggest that the SX-bodies contribute to the inhibition of protein synthesis upon exposure to NMDA by sequestering and/or degrading mRNAs.

RESULTS

We are interested in mRNA-silencing bodies putatively involved in the translational silencing that occurs at the post-synapse upon NMDAR stimulation. First, we defined the population of processing-body-related foci present at the post-synapses and focused on XRN1 particles. Then, we investigated whether the local changes in translational activity induced by synaptic stimulation correlate with their assembly or disassembly. Finally, we performed functional studies that suggest that the XRN-1-positive bodies are involved in translational silencing at the post-synapse.

XRN1 forms synaptic bodies that are different from processing bodies

We analyzed the subcellular distribution of selected processing body components in hippocampal neurons at 17 days *in vitro*. At this time in culture, neurons show mature dendritic spines and respond to specific paradigms of synaptic stimulation (Baez et al., 2011). We focused on XRN1, DCP1a, Ge-1/Hedls/RCD8/EDC4 (which is a decapping co-activator required for processing body integrity) and Rck/p54/DDX6 (a translational repressor and co-activator of decapping that is also required for processing body assembly). All of these processing body components formed puncta located in the cell soma and dendrites (Fig. 1A–G and data not shown), as described previously by us and others (Cougot et al., 2008; Zeitelhofer et al., 2008; Miller et al., 2009; Thomas et al., 2011). For all these molecules, the number of foci along dendrites was comparable. However, their presence at the synapses – identified by staining of the pre-synaptic molecule synapsin – was different. We considered a given body to be associated with a synapse when the synapsin cluster overlapped by >25% of its area. We found that whereas ~60% of the XRN1 bodies associated with the synapses (Fig. 1A), most DCP1a or Ge-1/Hedls/RCD8/EDC4 puncta localized at the dendritic shaft, and only 23% and 20% of them were found close to the synapsin clusters (Fig. 1B). Reciprocally, 40–70% of the synapses in hippocampal neurons contain XRN1 bodies in the surroundings; whereas the proportion of synapses with DCP1a or Ge-1/Hedls/RCD8/EDC4 was significantly lower (Fig. 1B,C). The presence of XRN1 was analyzed with two polyclonal antibodies (see Materials and Methods) and both antibodies detected a similar number of synaptic XRN1 clusters, no larger than 0.3–0.6 µm in diameter. Random colocalization of XRN1 granules with synapsin clusters was assessed as described in Materials and Methods. Briefly, we generated randomized images by strategies described previously (reviewed in Dunn et al., 2011) and found that the colocalization between XRN1 and synapsin was up to ten times higher than the random values, with highly significant *P*-values (Fig. 1D). Similarly, although much lower, the presence of DCP1a at the synapse was above the expected random colocalization and was statistically significant (Fig. 1D).

In addition, we found that, in dendrites, the XRN1 puncta showed a very low level of colocalization with DCP1a. Between 5 and 10% of the XRN1 particles contained DCP1a and only 6–10% of DCP1a-containing dendritic bodies contained XRN1 (Fig. 1E). Random colocalization for this pair was calculated as above and we found that it was lower than the experimental values (Fig. 1F). By contrast, half of the dendritic DCP1a bodies contained Ge-1/Hedls/RCD8/EDC4 and, conversely, 43% of Ge-1/Hedls/RCD8/EDC4 bodies contained DCP1a. The random colocalization for these pairs was much lower (Fig. 1G). The colocalization between XRN1 and DCP1a was much higher in the soma, where the puncta positive for these molecules colocalized almost completely, as reported previously (Cougot et al., 2008). For comparison, the colocalization between XRN1 and DCP1a was analyzed in U2OS cells. As expected, 93% of XRN1 bodies contained DCP1a and, conversely, 96% of the DCP1a bodies contained XRN1, Ge-1/Hedls/RCD8/EDC4 and Rck/p54/DDX6.

Journal of Cell Science (2015) 128, 1542–1554 doi:10.1242/jcs.163295

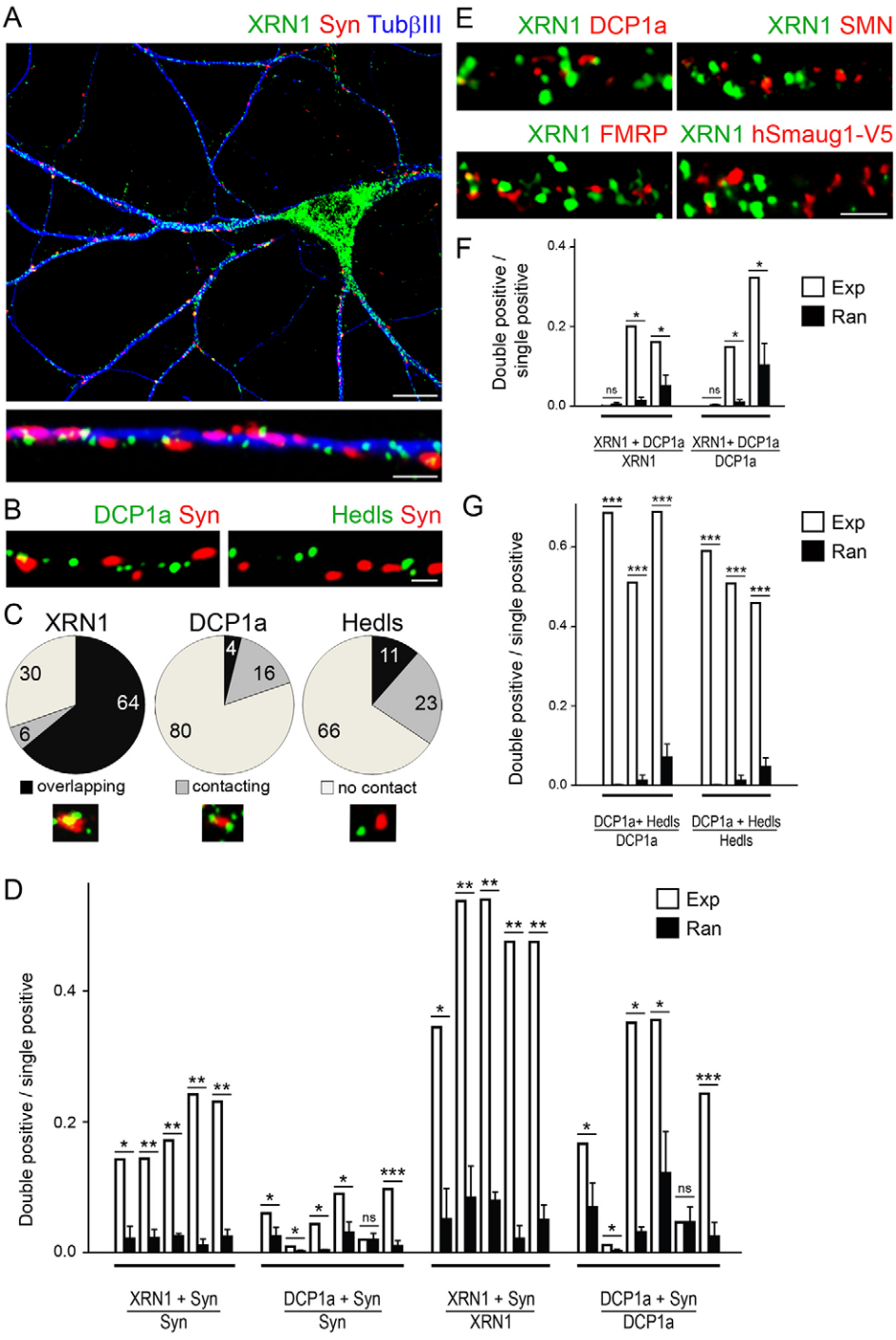

Fig. 1. XRN1 forms synaptic foci that are different from processing bodies. Hippocampal neurons were stained for tubulin βIII (TubβIII), the pre-synaptic component synapsin I (Syn) and XRN1 or the indicated molecules. (A) A representative magnification of a distal dendrite is depicted in the bottom panel. XRN1 foci are present at the synapses and in the dendritic shaft. (B) Foci of DCP1a or Ge-1/Hedls/RCD8/EDC4 in representative dendritic fragments. (C) Localization of the foci of XRN1, DCP1a or Ge-1/Hedls/RCD8/EDC4 relative to synapsin clusters. A synapse was considered to contain a given focus when the synapsin cluster overlapped more than 25% of the focus area. Examples of XRN1 foci overlapping or contacting synapsin clusters, or with no contact are depicted. In each case, 1000 synapses from 40 neurons on duplicate coverslips were analyzed. (D) Randomized images of representative dendritic fragments of ~15 µm in length stained for synapsin, XRN1 and DCP1a were generated as described in Materials and Methods. A minimum of seven randomized images was used in each case. The number of double- or single-stained pixels was analyzed by using ImageJ for each pair of molecules. The colocalization observed in each original micrograph (Exp) and the mean colocalization in the randomized images (Ran) is indicated as the fraction of double-stained pixels relative to single-stained pixels. (E) DCP1a, FMRP, SMN and transfected Smaug1/Samd4a tagged with V5 do not colocalize with XRN1. Representative dendritic fragments are depicted. Two independent transfection experiments yielded similar results. (F,G) Random colocalization between XRN1 and Dcp1a and between Dcp1a and Hedls was analyzed as in D. Scale bars: 10 µm (A, top), 2 µm (A, bottom), 1 µm (B,E). Data in D,F and G show the mean±s.d.; *$P \leq 0.05$; **$P \leq 0.001$; ***$P \leq 0.0001$; ns, not significant.

A population of small XRN1 foci lacking DCP1a was also present in U2OS cells (not depicted). The analysis of Ge-1/Hedls/RCD8/EDC4 and Rck/p54/DDX6 in the XRN1 bodies was not feasible as the primary antibodies against all these molecules were raised in rabbit. However, we speculate that these processing body components are scarcely present in the synaptic XRN1-positive puncta, as judged from the relatively lower abundance of Ge-1/Hedls/RCD8/EDC4 and Rck/p54/DDX6 in the vicinity of the synapse (Fig. 1C; data not shown). Thus, the XRN1 clusters located at the synapse are not canonical processing bodies, and we termed them synaptic XRN1-bodies (SX-bodies). Next, we investigated whether the XRN1-positive puncta contain FMRP, SMN or Smaug1/Samd4a, three important RBPs that are involved in RNA transport and localized translation, and we found that these markers did not significantly colocalize with XRN1. Only 6±2% (mean±s.d.) of the SX-bodies contained FMRP; 5±3% contained transfected hSmaug1-V5 and virtually none of them contained SMN (Fig. 1E).

The presence of XRN1 at the synapse was further analyzed in mouse hippocampal slices. We focused on the cornu ammonis (CA) region, specifically the CA1 and CA3 regions, which offer the possibility to visualize an ordered array of dendrites and synapses, respectively. Paralleling the distribution of XRN1 in cultured hippocampal neurons, XRN1 formed clusters of 0.3–

Journal of Cell Science (2015) 128, 1542–1554 doi:10.1242/jcs.163295

0.6 µm in diameter in CA1 dendrites. In addition, we found that ~60% of the synapses in the adult CA3 area contained XRN1-positive puncta (Fig. 2A,B). To confirm that XRN1 is associated with the post-synaptic side of the synapse, we fractionated hippocampal synaptoneurosomes (Sn) as described previously (Baez et al., 2011). We found that XRN1 co-purified with the post-synaptic density protein 95 (PSD95, also known as DLG4). Both molecules remained associated with the fraction enriched in post-synaptic components (PSD) and were excluded from the soluble fraction (Sol) enriched in the pre-synaptic marker synapsin (Fig. 2C). Collectively, these observations indicate that a large proportion of hippocampal dendritic spines contain XRN1 bodies that exclude decapping molecules, as well as FMRP, Smaug1/Samd4a and SMN, which would be involved in different regulatory pathways.

The SX-bodies behave like mRNA-silencing foci

We speculated that, like the processing bodies in most cell types, the XRN1-positive bodies contain repressed messengers that can resume translation. In this case, their presence should correlate inversely with polysome stabilization and should be affected by RNA breakdown, as is the case for processing bodies (Thomas et al., 2012). We investigated the response of the XRN1-bodies to cycloheximide, a polysome-stabilizing drug, and to puromycin, which provokes polysome disassembly. After a 10-minute exposure to cycloheximide, we found that both the size and the number of the XRN1-positive puncta decreased significantly, and they moderately increased upon a 10-minute treatment with puromycin. Both synaptic and extra-synaptic XRN1 bodies were similarly affected (Fig. 3A). Next, we treated live-permeabilized neurons with RNase as described previously (Thomas et al., 2012). We found that RNA digestion provoked a substantial loss of synaptic XRN1 puncta without affecting the synapsin patches (Fig. 3B). Collectively, these observations are compatible with the speculation that SX-bodies contain RNA and that they exchange transcripts directly with the polysomes or with some other cytosolic compartment in equilibrium with polysomes. In addition, this suggests that SX-body assembly involves pre-existing XRN1 molecules and that *de novo* protein synthesis is not required.

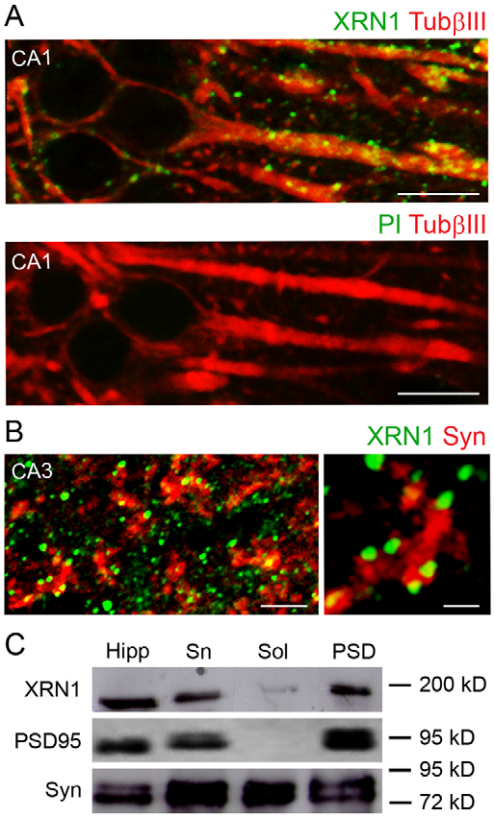

Fig. 2. Presence of XRN1 foci at the postsynapse. (A,B) XRN1, tubulin βIII (TubβIII) and the pre-synaptic component synapsin I (Syn) were stained in adult hippocampus slices, or rabbit preimmune serum (PI) was used. (A) A magnification of the CA1 region, including cell bodies and dendrites, is depicted. XRN1 puncta are detected along dendrites. (B) Magnification of the CA3 region showing the presence of several XRN1 foci associated with the synapses. Scale bars: 10 µm (A), 2 µm (B, left), 1 µm (B, right). (C) Synaptoneurosomes (Sn) isolated from adult hippocampus (Hipp) were separated into a soluble fraction (Sol) enriched in presynaptic components and that does not include PSD95, and a postsynaptic-density-enriched fraction (PSD). XRN1 co-purified with PSD95 in the PSD fractions, and both molecules are absent from the pre-synaptic fraction. A representative western blot out of three independent fractionations is depicted.

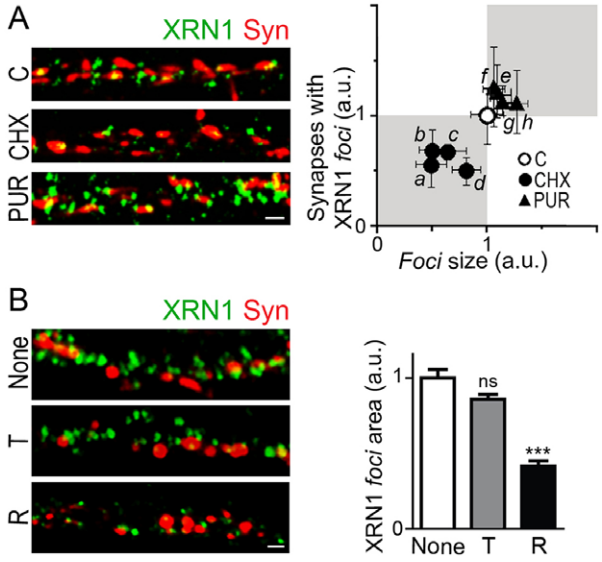

Fig. 3. SX-bodies are affected by translational inhibitors. (A) Neurons were exposed to cycloheximide (CHX) or puromycin (PUR) for 10 minutes, and the size and number of the SX-bodies were analyzed in 200 synapses from ten neurons for each treatment from duplicate coverslips. Values from four independent experiments normalized to those of untreated neurons are plotted. Cycloheximide affected the size (*a, b* and *c*, $P \leq 0.001$; *d*, not significant) and the number of the synaptic XRN1 puncta (*a, b, c* and *d*, $P \leq 0.001$), whereas puromycin affected the number (*e*, $P \leq 0.01$; *f*, $P \leq 0.001$; *g* and *h*, not significant) and elicited almost no effect on the size (*e, f* and *g*, not significant; *h*, $P \leq 0.05$, two-way ANOVA, Bonferroni post-test; $n=10$ neurons for each independent experiment). C, control; a.u. arbitrary units. (B) Live neurons were permeabilized with Triton X-100 (T) or permeabilized and then treated with RNase A (R) as indicated in Materials and Methods, and then fixed and stained for the indicated molecules. Representative dendritic fragments are shown. The presence of dendritic XRN1 bodies was evaluated in ten neurons from duplicate coverslips with a total of ~1400 µm dendrite length for each condition. The integrated area of the XRN1 puncta is plotted relative to control values. Scale bars: 1 µm. Error bars show s.e.m.;

Journal of Cell Science (2015) 128, 1542–1554 doi:10.1242/jcs.163295

The presence of synaptic XRN1 bodies inversely correlates with the protein synthesis rate, and NMDA reduces translation and enhances their formation

Next, we wondered whether the synaptic XRN1 bodies respond to synaptic stimulation in a manner that correlates with translational changes. In particular, we predicted that the decrease in mRNA translation upon NMDAR stimulation would be accompanied by an increased assembly of XRN1 bodies and/or some other mRNA-silencing foci. First, we monitored the local changes in the protein synthesis rate upon a short stimulation with 30 µM NMDA or 100 µM DHPG, which stimulates metabotropic receptors. We treated cultured hippocampal neurons with agonists as reported previously (Antar et al., 2004; Cougot et al., 2008; Park et al., 2008; Zeitelhofer et al., 2008; Baez et al., 2011; Tatavarty et al., 2012; Graber et al., 2013). We treated the neurons with tetrodotoxin (TTX), a drug that blocks voltage-gated sodium channels and spontaneous activity, and then we exposed the cells to a 5-minute pulse of 30 µM NMDA or 100 µM DHPG (see Materials and Methods). For *in situ* metabolic labeling of proteins, we used a recently described strategy termed fluorescent non-canonical amino acid tagging (FUNCAT) that has been used to monitor dendritic translation upon exposure to brain-derived neurotrophic factor (BDNF) (Dieterich et al., 2010) and, more recently, to show the reactivation of stalled polysomes upon treatment with DHPG (Graber et al., 2013). We labeled the proteins synthesized before the stimuli with L-azidohomoalanine (AHA) and the proteins synthesized during the 15 or 30 minutes after the stimulus with L-homopropargylglycine (HPG) (Fig. 4A). As expected, NMDAR stimulation provoked a reduction in the incorporation of HPG, indicating a reduced local translation rate (Fig. 4A,B; Baez et al., 2011). By contrast, a DHPG pulse increased the incorporation of HPG by a factor of two. These observations indicate that NMDA reduced and DHPG stimulated protein synthesis, which is compatible with previous reports using different experimental systems. Among other observations, dendritic translation evaluated with a transfected GFP-based reporter is stimulated by DHPG or by NMDAR blockers, and incorporation of amino acids is reduced in neurons exposed to short pulses of NMDA (Marin et al., 1997; Job and Eberwine, 2001; Sutton et al., 2004).

Next, we investigated whether the XRN1 puncta respond to NMDA or DHPG with changes in their number and/or size. As above, we treated the neurons with TTX before a short stimulation with NMDA or DHPG, and then transferred them to conditioned medium. Paralleling the differential effect on the protein synthesis rate, we found that the NMDA or DHPG pulses provoked opposite responses. Half an hour after stimulation, NMDA induced the appearance of new synaptic XRN1 puncta and their enlargement, whereas a DHPG pulse provoked their disappearance (Fig. 5A). In both cases, the size and number was significantly affected and, in subsequent experiments, we determined the total area of the XRN1-positive puncta at the synapses, relative to non-treated neurons, as indicated in Materials and Methods. We followed the response from immediately after the pulse up to 6 hours afterwards (Fig. 5B–F). The induction of synaptic XRN1 puncta triggered by NMDA was maximal at 30 minutes after the pulse and lasted for several hours. This timecourse roughly correlates with that of the protein synthesis inhibition triggered by NMDA (Fig. 4A). Conversely, the stimulation with DHPG provoked both an increase in protein synthesis and the disappearance of the synaptic XRN1 puncta with comparable timecourses (Fig. 4A; Fig. 5C–F). These observations

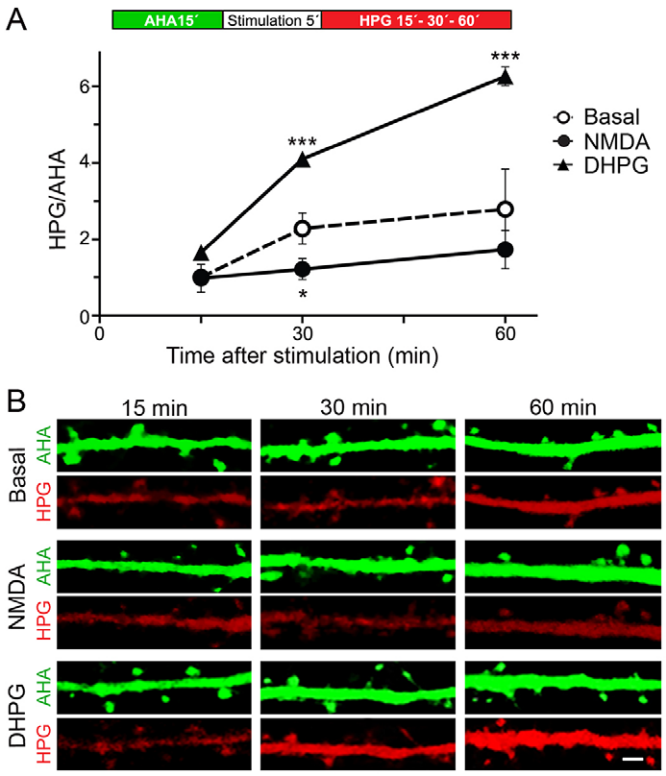

Fig. 4. NMDA and DHPG differentially affect the protein synthesis rate at dendrites. Sequential metabolic labeling of proteins with the substituted amino acids AHA and HPG was performed as indicated in Materials and Methods to evaluate dendritic protein synthesis before and after the stimulus. (A) The signal intensities were measured by confocal microscopy at the indicated times after stimulation and the ratio of HPG:AHA was calculated. Values normalized to the 15-minute time point of non-stimulated neurons (basal) are plotted. Mean values from three independent experiments are plotted, where 150 dendrite fragments from 20 neurons were evaluated in duplicate (total length, 1200 µm) for each time point and treatment. Error bars show s.e.m. Statistical significance for each treatment relative to non-stimulated neurons at each time point is indicated; *$P<0.05$; ***$P<0.001$ (two-way ANOVA, Bonferroni post-test). (B) Representative dendrite fragments depicting the incorporation of AHA (green) and HPG (red) at the

suggest that the assembly of the SX-bodies is linked to the repression of translation and their disassembly is linked to its activation. For comparison, we simultaneously analyzed the response of the S-foci and FMRP granules, which are linked to synaptic translation. The S-foci are synaptic mRNA-silencing foci that dissolve upon NMDAR stimulation, thus releasing transcripts and allowing their translation, and the FMRP-positive granules disassemble upon mGluR stimulation (Antar et al., 2004; Baez et al., 2011; Pascual et al., 2012; Graber et al., 2013). We found that the SX-bodies, the S-foci and the FMRP granules responded to synaptic stimulation with different patterns. Whereas the SX-bodies were induced upon NMDAR activation, showing significant changes at 30 minutes after stimulation, the S-foci immediately dissolved and the presence of FMRP-positive granules was almost unaffected by NMDA (Fig. 5B,D–F), as described previously (Antar et al., 2004; Baez et al., 2011). By contrast, the three types of foci disassembled upon DHPG stimulation, although with different kinetics. Whereas the dissolution of the S-foci and FMRP-positive granules was maximal immediately upon the DHPG pulse,

Journal of Cell Science (2015) 128, 1542–1554 doi:10.1242/jcs.163295

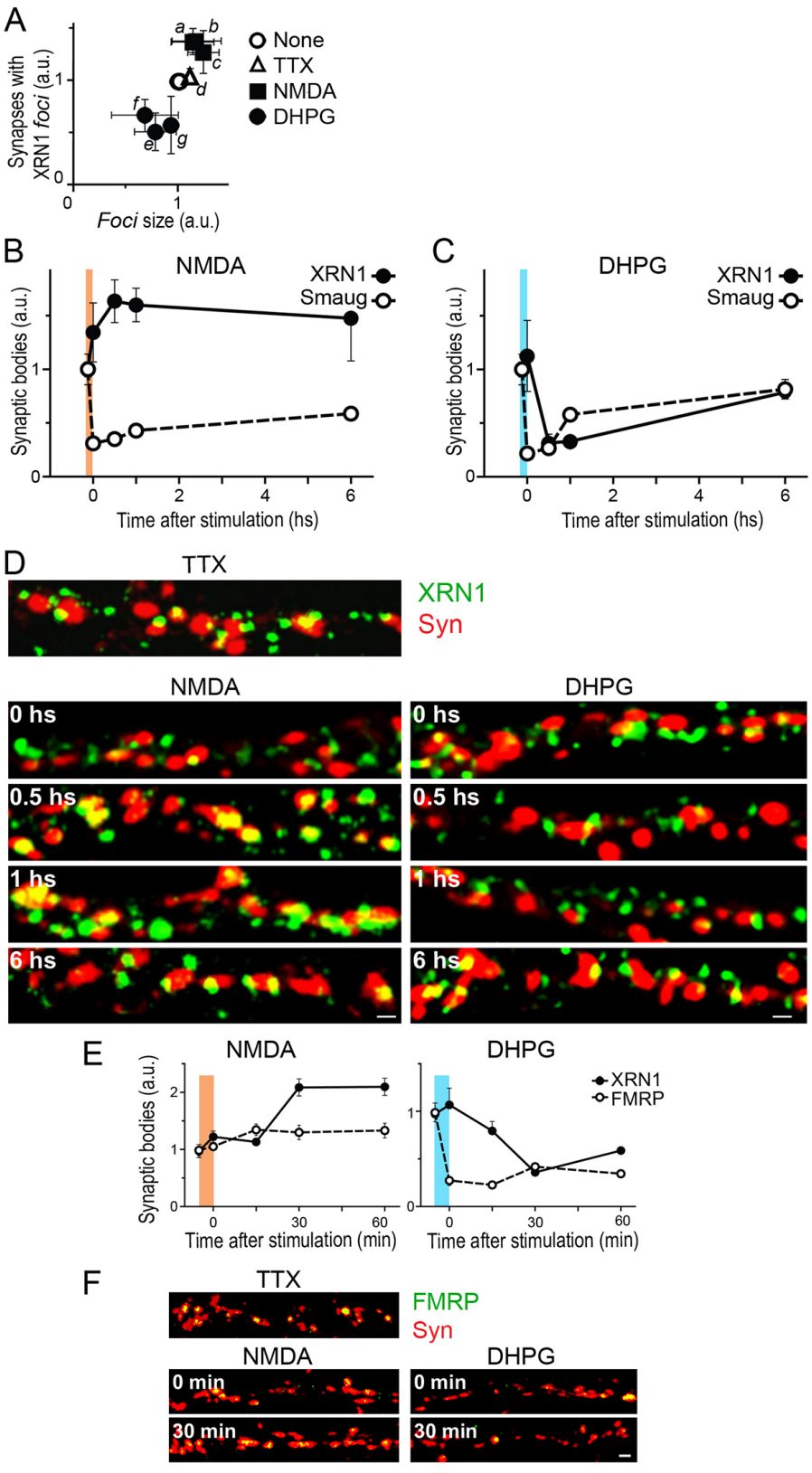

Fig. 5. SX-bodies, S-foci and FMRP granules respond differently to NMDA and DHPG stimulation. (A) The size and number of the synaptic XRN1 puncta were analyzed in untreated neurons (None), in neurons exposed to TTX for 16 hours and transferred to normal medium for 35 minutes (TTX), and in neurons exposed to TTX for 16 hours, pulsed for 5 minutes with NMDA or DHPG and transferred to normal medium for 30 minutes. Values normalized to those of TTX-treated cells without TTX withdrawal are depicted. NMDA and DHPG had opposite effects. Two hundred synapses from ten neurons from duplicate coverslips from three independent experiments were analyzed. Statistical significance for SX-body size and number relative to non-stimulated neurons was calculated by two-way ANOVA with Bonferroni post-test ($n=10$ neurons for each independent experiment) and was, respectively: *a*, $P\leq0.01$ and $P\leq0.001$; *b*, $P\leq0.01$ and $P\leq0.001$; *c*, $P\leq0.001$ and $P\leq0.001$; *d*, not significant for both size and number; *e*, $P\leq0.001$ and $P\leq0.001$; *f*, $P\leq0.001$ and $P\leq0.001$; *g*, not significant and $P\leq0.001$. a.u. arbitrary units. (B–F) Neurons were treated with TTX for 16 hours, exposed to NMDA or DHPG for 5 minutes and transferred to conditioned medium as above. The integrated area of the synaptic XRN1-positive bodies, of the S-foci stained with a specific antibody against Smaug1 and of FMRP-positive granules present at the synapses was analyzed and plotted normalized to that of TTX-treated neurons. For each protein, for each time point and treatment, a total of 500 synapses from ten neurons from duplicate coverslips were analyzed. A representative experiment out of three is depicted. Error bars show s.e.m. Scale bars: 1 μm.

the synaptic XRN1 bodies started to respond 15 minutes after stimulation with a maximal effect 30 minutes afterwards (Fig. 5C–F). At 6 hours after the DHPG pulse, both the SX-bodies and the S-foci recovered partially (Fig. 5C,D). We also analyzed the effect of NMDA and DHPG on the dendritic XRN1 and Smaug1 bodies located outside the synapses, which we termed extra-synaptic XRN1 and extra-synaptic Smaug1 bodies, respectively. We found that, as in the case of the bodies associated with synapses, NMDAR stimulation increased the number of extra-synaptic XRN1 bodies and reduced the number of extra-synaptic Smaug1 bodies

Journal of Cell Science (2015) 128, 1542–1554 doi:10.1242/jcs.163295

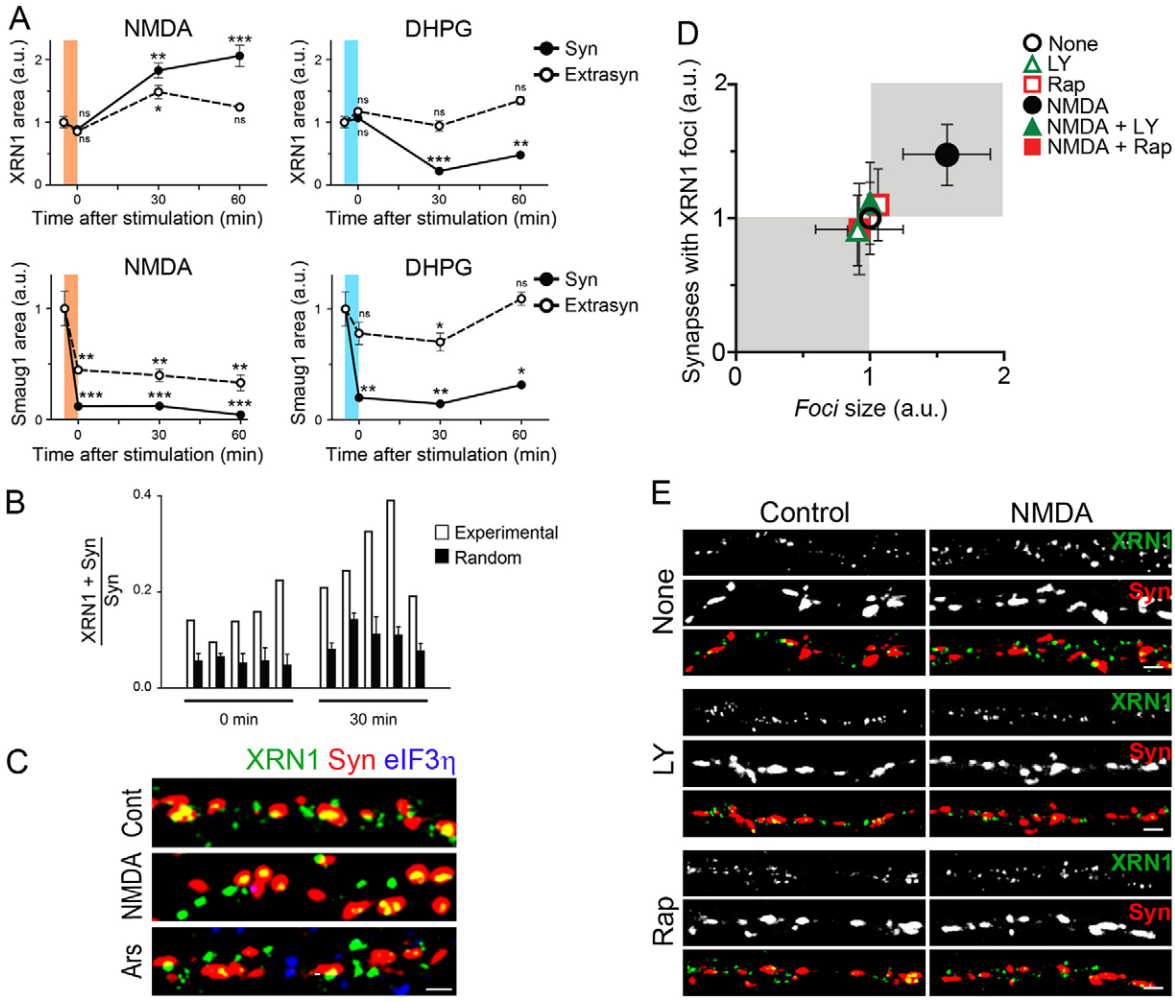

Fig. 6. NMDA and DHPG trigger mostly a local effect and the mTOR pathway regulates SX-body assembly upon NMDAR stimulation. (A) Cultured hippocampal neurons were exposed to NMDA or DHPG as described for Fig. 5 and stained for synapsin and XRN1 or for synapsin and Smaug1. The integrated area of the puncta associated with synapses (Syn) or not in contact with synapses (Extrasyn) was analyzed at the indicated time points. Values normalized to those of the TTX-treated neurons are plotted. a.u., arbitrary units. Error bars show s.e.m. *P≤0.05; **P≤0.001; ***P≤0.0001; ns, not significant (statistical significance relative to untreated neurons as determined by using one-way ANOVA with Bonferroni post-test). (B) Random colocalization for XRN1 and synapsin was analyzed in five representative dendritic fragments immediately after the NMDA pulse or 30 minutes after the pulse, as in Fig. 1. In all cases, P≤0.0001 in all pairs experimental versus random. Error bars show s.d. (C) Neurons were pulsed with NMDA for 5 minutes and transferred to conditioned medium for 60 minutes, or treated with arsenite (Ars) for 60 minutes, and the indicated molecules were immunostained. Ten randomly selected neurons were analyzed and the stress granule marker eIF3η was never detected in the XRN1 dendritic puncta. Cont, control. (D,E) Neurons were exposed to NMDA in the presence or absence of the PI3K inhibitor LY294002 (LY) or the mTOR inhibitor rapamycin (Rap). The size and number of XRN1-positive puncta at the synapse was evaluated 30 minutes after the pulse, as above. A total of 200 synapses from ten neurons randomly selected from duplicate coverslips were analyzed for each treatment. Error bars show s.e.m. Statistical significance relative to untreated neurons as determined by using one-way ANOVA with Bonferroni post-test (n=10 neurons for each independent experiment) was as follows: size and number upon NMDA treatment, P<0.0001 and P<0.05, respectively; all other cases, not significant. Scale bars: 1 μm.

(Fig. 6A). The effect of NMDA in extra-synaptic bodies was significant, but lower than the effect on the bodies close to synapses. In addition, DHPG had no effect on the extra-synaptic XRN1 bodies and moderately affected the extra-synaptic Smaug1 bodies (Fig. 6A), suggesting a local effect.

The exposure to NMDA increased the number and size of the XRN1 puncta and this increases the chances of random colocalization with synapses. We evaluated the contribution of the random colocalization between XRN1 and synapsin after NMDA stimulation as above. We found that, as in resting neurons, the expected random colocalization was significantly lower (P≤0.0001) than the experimental values (Fig. 6B). Collectively, all these observations indicate that the dynamics of the RNA granules containing XRN1, Smaug1 or FMRP are tightly controlled upon synapse stimulation.

Stress granules form during the translational silencing triggered by cellular stress, and XRN1 is recruited to stress granules under specific conditions (Thomas et al., 2009; Thomas et al., 2011). To investigate whether the XRN1 puncta induced concomitantly with the translational silencing triggered by NMDA are stress granules, we assessed the presence of the eukaryotic translation factor 3η (eIF3η, also known as EIF3B), a widely accepted stress granule marker. Stress granules were not detected at the synapses upon NMDAR stimulation and neither basal nor induced XRN1-positive puncta stained positive for eIF3η (Fig. 6C). For comparison, we treated the neurons with arsenite, a known inductor of oxidative stress. As expected, stress granules were

Journal of Cell Science (2015) 128, 1542–1554 doi:10.1242/jcs.163295

detected in the cell soma and dendrites upon the oxidative stress stimulus, and we found that they did not contain XRN1 (Fig. 6C, lower panel). Thus, the XRN1-positive bodies present in resting, NMDA-stimulated or stressed neurons were not stress granules.

Finally, we investigated whether the mTOR pathway is involved in SX-body dynamics. mTOR is activated upon NMDAR stimulation and mediates the repression of a number of messengers and the translational activation of others (Sosanya et al., 2013). We found that the pharmacological inhibition of mTOR or of the upstream kinase phosphoinositide 3-kinase (PI3K) with specific drugs blocked the formation of synaptic XRN1 puncta triggered by NMDA (Fig. 6D,E). Thus, local translation and SX-body dynamics are both under the control of the mTOR pathway, suggesting that they are coordinately regulated or linked in a cause–consequence relationship.

XRN1 contributes to the translational silencing upon NMDAR stimulation

The above experiments indicate that the SX-bodies behave as mRNA-silencing foci that form and grow in size when local protein synthesis is repressed. We speculated that the XRN1-positive bodies help the translational silencing elicited by NMDA, and we analyzed the effect of XRN1 knockdown with a specific siRNA pool (siXRN1). If the XRN1-positive bodies directly regulate translation, then XRN1 knockdown should attenuate the decrease in translation induced by NMDA.

First, we evaluated the efficiency of the XRN1 knockdown in cultured neurons. Western blot analysis indicated a significant reduction in XRN1 levels (Fig. 7A). In addition, the number of XRN1-positive puncta in synapses and in the dendritic shaft was reduced to half of the basal number (Fig. 7A). Then, we exposed the neurons to an NMDA pulse and analyzed the protein synthesis rate *in situ*, before and after the stimulus (see Fig. 4 above). As expected, NMDAR stimulation provoked a global reduction in the translation rate in the neurons treated with a control siRNA. At 30 minutes after the pulse, the incorporation of HPG was reduced to 0.53 (±0.06; $P=0.0036$; ±s.e.m.) relative to non-stimulated neurons. By contrast, XRN1-knockdown neurons showed a considerably weaker response and protein synthesis was not significantly reduced, as we found that the incorporation of HPG was 0.83 (±1.4; not significant) relative to control neurons (Fig. 7B,C). These results suggest that XRN1-positive bodies contribute to the local translational silencing elicited by NMDA, likely by masking or degrading transcripts.

DISCUSSION

Regulation of translation by synaptic activity is key to plasticity and homeostasis. NMDAR stimulation globally inhibits dendritic protein synthesis with consequences for translation specificity (reviewed in Thomas et al., 2014). Here, we show that the translational silencing upon exposure to NMDA is linked to the formation of synaptic XRN1-positive bodies, which are novel post-synaptic bodies that contain XRN1 and apparently lack decapping activity and that we termed SX-bodies. The SX-bodies are dynamic; their presence is affected by synaptic stimulation and inversely correlates with the local translational activity. Moreover, the disruption of the SX-bodies by XRN1 knockdown impaired the global translational repression triggered by NMDAR stimulation, suggesting that the SX-bodies contribute to mRNA silencing. These results open a number of questions.

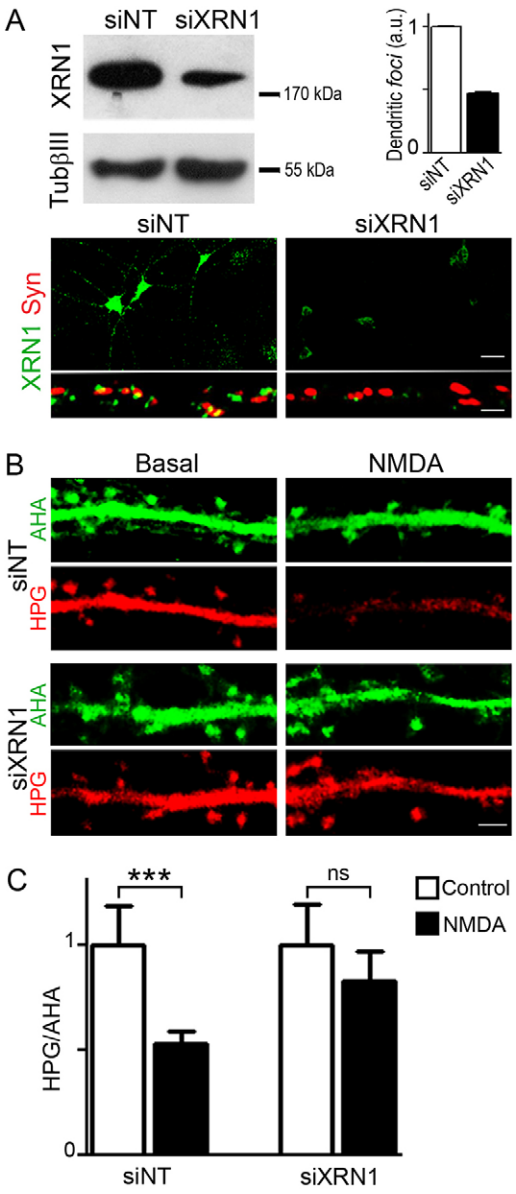

Fig. 7. The SX-bodies contribute to the repression of translation upon NMDAR activation. Neurons were treated with the indicated siRNAs as indicated in Materials and Methods. (A) XRN1 knockdown was confirmed by western blotting (left) and by immunofluorescence (right and bottom). The presence of XRN1-positive puncta was evaluated as above. a.u., arbitrary units. (B) siRNA-treated neurons were stimulated with NMDA and protein synthesis was visualized *in situ* as in Fig. 4. (C) The HPG:AHA ratio after a 30-minute stimulation was evaluated in representative dendritic fragments from 12 neurons from duplicate coverslips (total length, 700 µm). Mean values relative to those of non-stimulated neurons averaged from three independent experiments are plotted. Scale bars: 20 µm (A, upper panel); 1 µm (A, lower panel, B). Error bars show s.e.m. ***$P<0.001$; ns, not significant (one-way ANOVA with Bonferroni post test).

What is the nature of the SX-bodies?

We believe that these assemblages store or degrade mRNAs that are not being translated. Their disparate response to polysome stabilization or destabilization by specific drugs is comparable to that of processing bodies and stress granules, and we speculate that, similarly to processing bodies and stress granules, the SX-bodies contain repressed transcripts that might return to

Journal of Cell Science (2015) 128, 1542–1554 doi:10.1242/jcs.163295

translation. These observations and the sensitivity to RNase argue strongly against the possibility that the SX-bodies are mere XRN1 storage sites. We unsuccessfully attempted to detect RNA molecules in the SX-bodies by *in situ* hybridization strategies, and this is likely because mRNA masking in granules impairs detection (Buxbaum et al., 2014). Recent work indicates that RNA granules might contain stalled polysomes (Graber et al., 2013). This does not seem to be the case with the SX-bodies, as they exclude the initiation factor eIF3η and rapidly dissolve upon polysome stabilization by cycloheximide, which does not affect stalled polysomes (Graber et al., 2013). For the same reasons, we speculate that active translation is not possible in the SX-bodies, even though translation occurs in a number of ribonucleoparticle (RNP) granules (Tatavarty et al., 2012; Yasuda et al., 2013; Pimentel and Boccaccio, 2014).

Multiple studies support the notion that the formation of processing bodies and stress granules is the consequence and not the cause of the translational silencing (Eulalio et al., 2007; Buchan and Parker, 2009; Loschi et al., 2009; Thomas et al., 2011). However, RNA granule formation helps mRNA masking in dendrites, and the dissolution of related mRNA-silencing foci containing Smaug1 or Pumilio precedes translational activation in neurons and oocytes (Baez et al., 2011; Kotani et al., 2013; Buxbaum et al., 2014; Park et al., 2014). We propose that the SX-bodies mask mRNAs and that the regulation of SX-body dynamics directly affects their translation.

What are the molecular mechanisms for mRNA silencing in the SX-bodies?

The SX-bodies appear to exclude decapping activity, as they do not contain DCP1a, an obligate co-factor that activates the enzymatic subunit DCP2. Similarly, independent bodies containing Pacman or DCP1a are present in the *Drosophila* oocyte (Lin et al., 2008). Indirect evidence additionally indicates that the SX-bodies also lack the decapping co-activators Ge-1/Hedls/RCD8/EDC4 and Rck/p54/DDX6. All this suggests that the SX-bodies are unlikely to represent sites for the processing of decapped mRNAs, although additional decapping enzymes exist in several organisms that might bind and activate XRN1 (Li et al., 2011; Sinturel et al., 2012; Bossé et al., 2013). Similarly, only a small fraction of dendritic DCP1a foci contain XRN1 (this work and Cougot et al., 2008), indicating that 5′-3′ degradation is unlikely to occur in the DCP1a foci. Moreover, we speculate that decapping is not a major activity at the DCP1a foci, given that the molecular interaction of the decapping machinery with XRN1 is important for efficient decapping (Braun et al., 2012; Jonas and Izaurralde, 2013). We and others have found that NMDA or kainic acid induce the dissolution of dendritic DCP1a foci, whereas these stimuli enhance the formation of XRN1 bodies (this work; L.L. and G.L.B., unpublished; Cougot et al., 2008; Zeitelhofer et al., 2008). The disparate responses of dendritic foci containing XRN1 or DCP1a upon synaptic stimulation further indicate that decapping and 5′-3′ decay are not coordinated in these bodies, and all this strongly suggests that both types of bodies are dendritic mRNA storage compartments.

Besides decapping, the endonucleolytic cleavage linked to NMD or to RISC-mediated silencing generates 5′ monophosphorylated ends that might serve as XRN1 substrates (Lejeune et al., 2003; Gatfield and Izaurralde, 2004; Souret et al., 2004; Bagga et al., 2005; Eberle et al., 2009; Huntzinger and Izaurralde, 2011; Nagarajan et al., 2013). Both pathways involve processing bodies, are active at dendrites and are regulated by synaptic stimulation, opening the possibility that the SX-bodies are relevant to these mechanisms (Giorgi et al., 2007; Schratt, 2009; Hillebrand et al., 2010; Huang et al., 2012). *Arc/Arg3.1* mRNA, an important transcript activated at several levels upon synaptic stimulation is targeted to a NMD-related pathway termed translation-dependent decay (TDD) that might affect additional transcripts (Giorgi et al., 2007). Relevantly, recent work demonstrated that NMDAR stimulation induces the degradation of *Arc/Arg3.1* mRNA at activated synapses, opening the possibility of a role for XRN1 (Farris et al., 2014). Staufen-mediated decay (SMD) is an additional pathway for regulated mRNA degradation, and RNA granules containing Staufen1 and Staufen2 are abundant in dendrites (Zeitelhofer et al., 2008; Park and Maquat, 2013). Relevantly, the NMD, TDD and SMD pathways involve Upf proteins, which directly interact with XRN1 (Nagarajan et al., 2013). Whether dendritic mRNAs cleaved by NMD, TDD, SMD or RISC are further processed in the SX-bodies remains to be investigated. Among other possible targets, degradation of mRNAs coding for translational activators might provide a link between XRN1 and the control of protein synthesis upon NMDAR stimulation.

However, our results are more compatible with a role for the SX-bodies in mRNA storage. In this model, XRN1 catalytic activity would not be involved and mRNAs resistant to 5′-3′ decay would be released in a regulated manner from the SX-bodies (Fig. 8A). XRN1 is a large molecule and the catalytic domain and additional protein regions required for degradative activity span only two thirds of its length, opening the possibility of additional molecular functions (Chang et al., 2011; Braun et al., 2012; Nagarajan et al., 2013). Remarkably, XRN1 displays several short regions enriched in lysine and/or glutamic acid (Fig. 8B), speculatively linked to RNA binding (Castello et al., 2012; Kramer et al., 2014). It is also relevant that proteins from the XRN1 family affect selected mRNAs, and transcripts carrying G-quartets – which are important motifs in dendritic mRNAs – are preferentially bound by mammalian XRN1 (Bashkirov et al., 1997; Darnell et al., 2001), all these putatively providing mechanisms for selective storage.

We propose that the XRN1-dependent pathway for mRNA silencing is enhanced upon NMDAR activation and weakened upon DHPG stimulation (Fig. 8A). NMDAR activation bidirectionally affects dendritic translation through multiple pathways. NMDAR stimulation provokes the translational repression of the voltage-gated potassium channel Kv1.1 by miR-129 and the mTOR pathway, which we found mediates SX-body formation (Raab-Graham et al., 2006; Sosanya et al., 2013). In addition, NMDA impairs elongation through the phosphorylation of the eukaryotic elongation factor 2, with a differential effect on specific transcripts and a global decrease in the protein synthesis rate (Marin et al., 1997; Sutton et al., 2006; Sutton et al., 2007). Whether miRNA-mediated repression or elongation inhibition are linked to SX-body formation is currently unknown. Likewise, whether mRNA silencing in the SX-bodies affects the translational activation of NMDAR-dependent transcripts remains to be explored.

How are the SX-bodies regulated?

Our observations underscore a novel repression pathway that involves the interaction of messenger molecules with XRN1 in specific cellular microdomains. The assembly of RNA granules, processing bodies and stress granules, as well as their dissolution, are currently conceptualized as phase-transition processes (Brangwynne, 2013; Hubstenberger et al., 2013; Jonas and Izaurralde, 2013; Toretsky and Wright, 2014), and

Journal of Cell Science (2015) 128, 1542–1554 doi:10.1242/jcs.163295

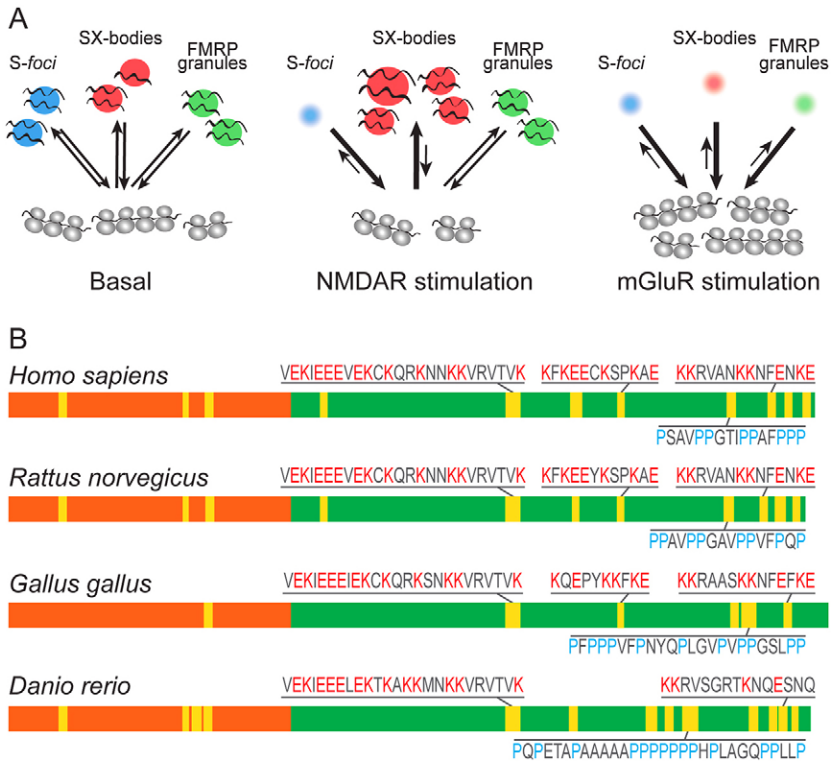

Fig. 8. Summary and model for SX-body dynamics. (A) Our observations indicate that NMDAR stimulation downregulates protein synthesis and induces the formation of the SX-bodies, which help translational silencing. Simultaneously, the S-foci dissolve, releasing transcripts to allow their translation. FMRP granules are not affected upon NMDA, but rapidly dissolve or remodel upon mGluR stimulation, likely releasing polysome stalling or other mechanisms for translation repression. The SX-bodies respond in a second wave and slowly dissolve upon mGluR activation, speculatively allowing the translation of masked transcripts. The S-foci are affected by DHPG in a similar manner. Multiple mRNA species are silenced upon NMDAR activation, and the identity of the transcripts masked in the SX-bodies remains unknown. See Discussion for details. (B) Structure of mammalian XRN1. The catalytic domain (orange boxes) in human XRN1 (NP_061874) spans amino acids 1–595, and a conserved region up to amino acid 1174 is additionally required for enzymatic activity (Chang et al., 2011, reviewed in Nagarajan et al., 2013). A region that binds the decapping machinery is located at the C-terminal 30 amino acids (not depicted) (Braun et al., 2012). Short LCRs (yellow boxes) are abundant in the C-terminal part. Stretches rich in Glu and/or Lys or with high proline content, putatively involved in RNA binding and protein aggregation, are indicated. These features are conserved in the rat, chicken and zebrafish molecules (XP_002730002.1, XP_422596.3 and NP_957327.2, respectively). Schemes are drawn to scale and human XRN1 spans 1706 residues.

we believe that the dynamics of the SX-bodies are under similar rules. According to this model, all these bodies behave as liquid droplets of ribonucleoparticles (RNPs) that dynamically exchange molecules with the cytosol. Phase transitions of RNP liquid droplets are controlled by changes in the local concentrations of their components, and we found that the availability of non-polysomal mRNA affects the size and the number of the SX-bodies. RNA molecules might contribute to the stability of RNP liquid droplets by serving as a platform for multiple binding, and we found that RNA breakdown affects SX-body integrity. Additional cohesive forces that might help the condensation of RNP liquid droplets depend on homotypic and heterotypic protein–protein interaction mediated largely by low complexity regions (LCRs) (Han et al., 2012; Kato et al., 2012; Brangwynne, 2013; Jonas and Izaurralde, 2013; Thomas et al., 2014). The XRN1 C-terminus displays several LCRs, some of them rich in proline, and we speculate that these LCRs are likely to play a role in SX-body aggregation (Fig. 8B). How the mTOR pathway affects SX-body aggregation and whether post-translational modifications influence XRN1 stabilization or degradation remains to be investigated. In addition, whether other proteins present in the SX-bodies contribute to their formation is currently unknown. So far, we found that several important RBPs that form granules – namely FMRP, Smaug1 and SMN – are excluded from the SX-bodies. Finally, condensation of liquid droplets is influenced by several physicochemical parameters, as well as by constraints imposed by the cytoskeleton network and molecular crowding (Brangwynne, 2013). Modulation of these factors by neuronal activity provides additional mechanisms for the regulated formation of SX-bodies and other RNP assemblages.

In addition to SX-body aggregation, translational regulation upon exposure to NMDA is accompanied by the dissolution of the S-foci and DCP1a foci, with the apparent release of CaMKII mRNA and other messengers yet to be identified (Cougot et al., 2008; Zeitelhofer et al., 2008; Baez et al., 2011). These responses are specific to NMDAR stimulation, and mGluR activation generates a different pattern. The SX-bodies, the S-foci and the FMRP granules dissolve upon mGluR stimulation with different timecourses, likely to allow the ordered translation of specific messengers. We propose that the concerted assembly and disassembly of different RNP liquid droplets increases translational diversity in response to different synaptic inputs (Fig. 8A).

MATERIALS AND METHODS

Neuron culture, siRNA treatment and plasmid transfection

All experiments involving animals were conducted according to the protocols approved by the Institutional Animal Care and Use Committee (IACUC) of the Fundación Instituto Leloir. Hippocampal cultures were prepared as described previously (Baez et al., 2011). Briefly, hippocampi were dissected from Sprague Dawley rats at embryonic day 18 and digested with trypsin. Cells were seeded on poly-D-lysine-coated glass coverslips (Sigma-Aldrich) and maintained at 5% CO_2 in Neurobasal medium (NB) supplemented with B27 and glutamine (complete NB), all reagents and nutrients from Invitrogen. All experiments were performed at 17 days *in vitro* unless otherwise indicated. For siRNA treatment, neurons were allowed to grow for 6 days *in vitro*, incubated with 100 nM siRNA complexed with Lipofectamine 2000 Transfection Reagent (Invitrogen) for 4 hours, and analyzed at 10 days afterwards unless otherwise indicated. A pool of four double-stranded (ds)RNAs (5′-CUA-AAGAAACUGCGGCUAU-3′, 5′-GAACAUACUACAUGACGAA-3′, 5′-CCAAAGAGGCGUAGACUCA-3′ and 5′-GCUCACAGGUCGUA-GAUAU-3′) against rat XRN1 (L-080615-01-0010) or a non-targeting pool of siRNAs (siNT) (D-001810-10); both from Dharmacon, Chicago, IL, were used. Plasmid transfection was performed 3 days after plating using Lipofectamine 2000 Transfection Reagent.

Cycloheximide and puromycin (Sigma-Aldrich) were used at 250 µg/ml and neurons were exposed for 10 minutes. Treatment with 100 µg/ml RNase A (Sigma) in conditioned complete NB was performed for

5 minutes after a 5-minute permeabilization with 0.1% Triton X-100 in conditioned complete NB, as described previously (Thomas et al., 2012). In all cases, stock solutions were diluted into complete NB medium.

Neuron stimulation and metabolic labeling of proteins

Before synaptic stimulation, neurons were exposed for 16 hours to 1 µM TTX (Tocris Bioscience). Stimulation with 30 µM NMDA (Sigma-Aldrich) or 100 µM DHPG (Tocris Bioscience) for 5 minutes and recovery in complete NB were performed as described previously (Baez et al., 2011). For metabolic labeling of proteins, neurons were treated for 16 hours with TTX in complete NB and incubated for 30 minutes in methionine-free DMEM (Sigma-Aldrich) plus TTX. Then, 1 mM AHA was added for 15 minutes. After a 5-minute pulse with NMDA, cells were incubated with 1 mM HPG for the indicated times in methionine-free DMEM (Sigma-Aldrich). After fixation and permeabilization, cells were incubated with Alexa-Fluor-488–alkyne [Alexa Fluor 488 5-carboxamido-(propargyl), bis (triethylammonium salt)], which reacts with the AHA azide group, and then with Alexa-Fluor-594–azide [Alexa Fluor 594 carboxamido-(6-azidohexanyl) bis(triethylammonium salt)], which reacts with the alkyne group of HPG-bearing proteins. All reagents were from Invitrogen. Signal intensity was measured by confocal microscopy in dendrite fragments located at 50 µm or more from the soma to minimize the contribution from proteins delivered from the cell body (Dieterich et al., 2010).

Immunofluorescence

Immunofluorescence of cultured cells was performed after fixation, permeabilization and blocking as usual (Baez et al., 2011; Thomas et al., 2012). Primary antibodies were diluted as follows: rabbit anti-mammalian XRN1 used in Fig. 1A,D; Fig. 2A–C; Fig. 3A,B; Fig. 5A–F; Fig. 6 and Fig. 7A (Bethyl Laboratories), 1:100; rabbit anti-mammalian XRN1 provided by Jens Lykke-Andersen (Division of Biological Sciences, University of California, San Diego, USA), 1:100; anti-Smaug1/Samd4a prepared in our laboratory, 1:500 (Baez and Boccaccio, 2005); monoclonal IgG2a anti-DCP1a (Abnova Corporation), 1:1000; polyclonal rabbit anti-Ge-1/Hedls/RCD8/EDC4 or anti Rck/p54 (Bethyl Laboratories, Inc.), 1:500; IgG2b anti-tubulin βIII (Sigma-Aldrich), 1:500; IgG1 anti-synapsin I (Synaptic Systems), 1:100; IgG2b anti-FMRP, clone 7G1-1 (Developmental Studies Hybridoma Bank), 1:50; and goat anti-eIF3η N-20 (Santa Cruz), 1:250; anti-V5 (Invitrogen), 1:500. Secondary antibodies coupled to Alexa Fluor 488, Alexa Fluor 555 or Alexa Fluor 666 (Invitrogen) were used at 1:500–1:1000. Secondary antibodies coupled to Cy2, Cy3 or Cy5 (Jackson ImmunoResearch Laboratories, Inc.) were used at 1:300–1:500.

Brain sections, provided by Alejandro Schinder (Fundación Instituto Leloir, Argentina) and Alberto J. Ramos (University of Buenos Aires, Argentina) were stained following a free-floating method, as described previously. Briefly, after antigen retrieval by treatment at 95℃ for 5 minutes, sections were blocked in 10% normal donkey serum in PBS containing 0.3% Triton X-100, and incubated overnight with anti-XRN1 (1:100), anti-synapsin (1:200) and anti-tubulin βIII (1:200) at 4℃. The secondary antibodies donkey anti-rabbit-IgG and anti-mouse-IgG1 or -IgG2b (Jackson ImmunoResearch Laboratories, Inc.) were used at 1:250. Sections were mounted in PVA-Dabco (Sigma-Aldrich).

Image analysis

Images were acquired with a PASCAL-LSM or a LSM510 Meta confocal microscopes (Carl Zeiss), using C-Apochromat 40×/1.2 W Corr or 63×/1.2 W Corr water-immersion objectives for the LSM, and an EC Plan-Neofluor 40×/1.30 NA oil or Plan-Apochromat 63×/1.4 NA oil objectives for the LSM510 Meta. Images were acquired with LSM software (Carl Zeiss), and pixel intensity was always lower that 250 (saturation level is 255). Equipment adjustment was assessed by using 1-µm FocalCheck fluorescent microspheres (Invitrogen). Images were randomly selected for sampling, using the MAP2 or synapsin immunostaining or the AHA signal to select the dendritic fragments to be analyzed. No filters or gamma adjustments were used prior to the analysis of the size, number or intensity of the objects, which was performed with the ImageJ software. A synapse was considered to be positive when a focus overlapped at least 25% with the synapsin I patch. The area of the foci associated with synapses was measured with ImageJ and a value of zero was assigned to negative synapses.

Random colocalization of granules and synapses was evaluated by using methods described previously (reviewed in Dunn et al., 2011). The channel corresponding to XRN1, DCP1a or Ge-1/Hedls/RCD8/EDC4 was randomized by block scrambling or displacement along the dendritic axis. The use of blocks larger than the particles to be analyzed is recommended, and we split dendritic fragments into segments of 4 µm length, and reconstructed images randomized along the dendrite axis. Randomization by displacement of one channel relative to the other is obtained when the shift is above a minimal distance that depends on the size of the objects. Here, we restricted the displacement along the dendritic axes (x-axis), and analyzed the randomized images generated by 4, 8 or 10-µm displacements. In all cases, the randomized images were visually inspected to check that the granules did not localize in the extracellular space, and when possible, images were adjusted with minimal displacements along the y-axis or a 180° rotation to fit all pixels inside the dendrite area. Single and double-labeled pixels were analyzed by ImageJ.

Hippocampus fractionation

Hand-dissected hippocampi from adult mice were fractionated as described previously (Baez et al., 2011). Briefly, a crude synaptosome preparation was extracted in 2% Triton X-100 pH 6, followed by 1% Triton X-100 pH 8.0, to obtain a fraction enriched in soluble presynaptic components and a fraction containing postsynaptic densities and insoluble presynaptic proteins.

Western blotting

Western blotting was performed by standard procedures using Immobilon-P polyvinylidene difluoride membranes (Millipore), ECL Prime (GE Healthcare) and Hyperfilm (GE Healthcare). Primary antibodies were used as follows: rabbit anti-XRN1, diluted 1:5000; anti-PSD95 (Upstate Technologies), 1:1000; anti-synapsin I (Synaptic Systems), 1:5000. Secondary antibodies conjugated to peroxidase (Sigma) were used at 1:5000.

Statistics

Each experimental point includes duplicates or triplicates, as indicated. P-values relative to control treatments according to two-way ANOVA or the indicated test were determined using Instat software (GraphPad Software, Inc.). The number of synapses, neurons and dendritic lengths analyzed are indicated for each case.

Acknowledgements

We thank the members of G.L.B.'s laboratory for their constant support and fruitful discussions, and M.V. Baez and M.L. Pascual for advice and help in the preparation of primary neurons. We are grateful to A. Schinder and V. Piatti (FIL) and A.J. Ramos and F. Angelo (UBA) for kindly providing tissue sections, to M. Neme (FIL) for assistance in confocal microscopy analysis and to J. Lykke-Andersen for providing antibodies.

Competing interests

The authors declare no competing or financial interests.

Author contributions

L.L. performed and analyzed experiments; M.G.T. performed and analyzed experiments and contributed to the writing; G.L.B. conceived and supervised the project, analyzed data and wrote the manuscript.

Funding

This work was supported by the following grants: PICT 2011-1301 and PICT 2010-1850 to G.L.B.; PICT 2010-2339, PICT 2012-2493 and PIP 205-2011-2013 to M.G.T. M.G.T. and G.L.B. are investigators from the Agencia Nacional de Promoción Científica y Tecnológica (ANPCyT) and from Consejo Nacional de Investigaciones Científicas y Tócnicas (CONICET). L.L. was supported by fellowships from the University of Buenos Aires and CONICET.

References

Antar, L. N., Afroz, R., Dictenberg, J. B., Carroll, R. C. and Bassell, G. J. (2004). Metabotropic glutamate receptor activation regulates fragile x mental retardation protein and FMR1 mRNA localization differentially in dendrites and at synapses. *J. Neurosci.* **24**, 2648-2655.

Baez, M. V. and Boccaccio, G. L. (2005). Mammalian Smaug is a translational repressor that forms cytoplasmic foci similar to stress granules. *J. Biol. Chem.* **280**, 43131-43140.

Baez, M. V., Luchelli, L., Maschi, D., Habif, M., Pascual, M., Thomas, M. G. and Boccaccio, G. L. (2011). Smaug1 mRNA-silencing foci respond to NMDA and modulate synapse formation. *J. Cell Biol.* **195**, 1141-1157.

Bagga, S., Bracht, J., Hunter, S., Massirer, K., Holtz, J., Eachus, R. and Pasquinelli, A. E. (2005). Regulation by let-7 and lin-4 miRNAs results in target mRNA degradation. *Cell* **122**, 553-563.

Banko, J. L., Hou, L., Poulin, F., Sonenberg, N. and Klann, E. (2006). Regulation of eukaryotic initiation factor 4E by converging signaling pathways during metabotropic glutamate receptor-dependent long-term depression. *J. Neurosci.* **26**, 2167-2173.

Bashkirov, V. I., Scherthan, H., Solinger, J. A., Buerstedde, J. M. and Heyer, W. D. (1997). A mouse cytoplasmic exoribonuclease (mXRN1p) with preference for G4 tetraplex substrates. *J. Cell Biol.* **136**, 761-773.

Bossé, G. D., Rüegger, S., Ow, M. C., Vasquez-Rifo, A., Rondeau, E. L., Ambros, V. R., Grosshans, H. and Simard, M. J. (2013). The decapping scavenger enzyme DCS-1 controls microRNA levels in Caenorhabditis elegans. *Mol. Cell* **50**, 281-287.

Brangwynne, C. P. (2013). Phase transitions and size scaling of membrane-less organelles. *J. Cell Biol.* **203**, 875-881.

Braun, J. E., Truffault, V., Boland, A., Huntzinger, E., Chang, C. T., Haas, G., Weichenrieder, O., Coles, M. and Izaurralde, E. (2012). A direct interaction between DCP1 and XRN1 couples mRNA decapping to 5′ exonucleolytic degradation. *Nat. Struct. Mol. Biol.* **19**, 1324-1331.

Buchan, J. R. and Parker, R. (2009). Eukaryotic stress granules: the ins and outs of translation. *Mol. Cell* **36**, 932-941.

Buxbaum, A. R., Wu, B. and Singer, R. H. (2014). Single β-actin mRNA detection in neurons reveals a mechanism for regulating its translatability. *Science* **343**, 419-422.

Castello, A., Fischer, B., Eichelbaum, K., Horos, R., Beckmann, B. M., Strein, C., Davey, N. E., Humphreys, D. T., Preiss, T., Steinmetz, L. M. et al. (2012). Insights into RNA biology from an atlas of mammalian mRNA-binding proteins. *Cell* **149**, 1393-1406.

Chang, J. H., Xiang, S., Xiang, K., Manley, J. L. and Tong, L. (2011). Structural and biochemical studies of the 5′→3′ exoribonuclease Xrn1. *Nat. Struct. Mol. Biol.* **18**, 270-276.

Cougot, N., Bhattacharyya, S. N., Tapia-Arancibia, L., Bordonné, R., Filipowicz, W., Bertrand, E. and Rage, F. (2008). Dendrites of mammalian neurons contain specialized P-body-like structures that respond to neuronal activation. *J. Neurosci.* **28**, 13793-13804.

Darnell, J. C., Jensen, K. B., Jin, P., Brown, V., Warren, S. T. and Darnell, R. B. (2001). Fragile X mental retardation protein targets G quartet mRNAs important for neuronal function. *Cell* **107**, 489-499.

Darnell, J. C., Van Driesche, S. J., Zhang, C., Hung, K. Y., Mele, A., Fraser, C. E., Stone, E. F., Chen, C., Fak, J. J., Chi, S. W. et al. (2011). FMRP stalls ribosomal translocation on mRNAs linked to synaptic function and autism. *Cell* **146**, 247-261.

di Penta, A., Mercaldo, V., Florenzano, F., Munck, S., Ciotti, M. T., Zalfa, F., Mercanti, D., Molinari, M., Bagni, C. and Achsel, T. (2009). Dendritic LSm1/CBP80-mRNPs mark the early steps of transport commitment and translational control. *J. Cell Biol.* **184**, 423-435.

Dieterich, D. C., Hodas, J. J., Gouzer, G., Shadrin, I. Y., Ngo, J. T., Triller, A., Tirrell, D. A. and Schuman, E. M. (2010). In situ visualization and dynamics of newly synthesized proteins in rat hippocampal neurons. *Nat. Neurosci.* **13**, 897-905.

Dunn, K. W., Kamocka, M. M. and McDonald, J. H. (2011). A practical guide to evaluating colocalization in biological microscopy. *Am. J. Physiol.* **300**, C723-C742.

Eberle, A. B., Lykke-Andersen, S., Mühlemann, O. and Jensen, T. H. (2009). SMG6 promotes endonucleolytic cleavage of nonsense mRNA in human cells. *Nat. Struct. Mol. Biol.* **16**, 49-55.

Eulalio, A., Behm-Ansmant, I., Schweizer, D. and Izaurralde, E. (2007). P-body formation is a consequence, not the cause, of RNA-mediated gene silencing. *Mol. Cell. Biol.* **27**, 3970-3981.

Farris, S., Lewandowski, G., Cox, C. D. and Steward, O. (2014). Selective localization of arc mRNA in dendrites involves activity- and translation-dependent mRNA degradation. *J. Neurosci.* **34**, 4481-4493.

Gatfield, D. and Izaurralde, E. (2004). Nonsense-mediated messenger RNA decay is initiated by endonucleolytic cleavage in Drosophila. *Nature* **429**, 575-578.

Giorgi, C., Yeo, G. W., Stone, M. E., Katz, D. B., Burge, C., Turrigiano, G. and Moore, M. J. (2007). The EJC factor eIF4AIII modulates synaptic strength and neuronal protein expression. *Cell* **130**, 179-191.

Graber, T. E., Hébert-Seropian, S., Khoutorsky, A., David, A., Yewdell, J. W., Lacaille, J. C. and Sossin, W. S. (2013). Reactivation of stalled polyribosomes in synaptic plasticity. *Proc. Natl. Acad. Sci. USA* **110**, 16205-16210.

Han, T. W., Kato, M., Xie, S., Wu, L. C., Mirzaei, H., Pei, J., Chen, M., Xie, Y., Allen, J., Xiao, G. et al. (2012). Cell-free formation of RNA granules: bound RNAs identify features and components of cellular assemblies. *Cell* **149**, 768-779.

Hillebrand, J., Pan, K., Kokaram, A., Barbee, S., Parker, R. and Ramaswami, M. (2010). The Me31B DEAD-Box helicase localizes to postsynaptic foci and regulates expression of a CaMKII reporter mRNA in dendrites of Drosophila olfactory projection neurons. *Front. Neural Circuits* **4**, 121.

Huang, Y. W., Ruiz, C. R., Eyler, E. C., Lin, K. and Meffert, M. K. (2012). Dual regulation of miRNA biogenesis generates target specificity in neurotrophin-induced protein synthesis. *Cell* **148**, 933-946.

Hubstenberger, A., Noble, S. L., Cameron, C. and Evans, T. C. (2013). Translation repressors, an RNA helicase, and developmental cues control RNP phase transitions during early development. *Dev. Cell* **27**, 161-173.

Huntzinger, E. and Izaurralde, E. (2011). Gene silencing by microRNAs: contributions of translational repression and mRNA decay. *Nat. Rev. Genet.* **12**, 99-110.

Ingelfinger, D., Arndt-Jovin, D. J., Lührmann, R. and Achsel, T. (2002). The human LSm1-7 proteins colocalize with the mRNA-degrading enzymes Dcp1/2 and Xrnl in distinct cytoplasmic foci. *RNA* **8**, 1489-1501.

Job, C. and Eberwine, J. (2001). Identification of sites for exponential translation in living dendrites. *Proc. Natl. Acad. Sci. USA* **98**, 13037-13042.

Jonas, S. and Izaurralde, E. (2013). The role of disordered protein regions in the assembly of decapping complexes and RNP granules. *Genes Dev.* **27**, 2628-2641.

Jones, C. I., Zabolotskaya, M. V. and Newbury, S. F. (2012). The 5′ → 3′ exoribonuclease XRN1/Pacman and its functions in cellular processes and development. *Wiley Interdiscip. Rev. RNA* **3**, 455-468.

Jones, C. I., Grima, D. P., Waldron, J. A., Jones, S., Parker, H. N. and Newbury, S. F. (2013). The 5′-3′ exoribonuclease Pacman (Xrn1) regulates expression of the heat shock protein Hsp67Bc and the microRNA miR-277-3p in Drosophila wing imaginal discs. *RNA Biol.* **10**, 1345-1355.

Kato, M., Han, T. W., Xie, S., Shi, K., Du, X., Wu, L. C., Mirzaei, H., Goldsmith, E. J., Longgood, J., Pei, J. et al. (2012). Cell-free formation of RNA granules: low complexity sequence domains form dynamic fibers within hydrogels. *Cell* **149**, 753-767.

Kotani, T., Yasuda, K., Ota, R. and Yamashita, M. (2013). Cyclin B1 mRNA translation is temporally controlled through formation and disassembly of RNA granules. *J. Cell Biol.* **202**, 1041-1055.

Kramer, K., Sachsenberg, T., Beckmann, B. M., Qamar, S., Boon, K. L., Hentze, M. W., Kohlbacher, O. and Urlaub, H. (2014). Photo-cross-linking and high-resolution mass spectrometry for assignment of RNA-binding sites in RNA-binding proteins. *Nat. Methods* **11**, 1064-1070.

Lejeune, F., Li, X. and Maquat, L. E. (2003). Nonsense-mediated mRNA decay in mammalian cells involves decapping, deadenylating, and exonucleolytic activities. *Mol. Cell* **12**, 675-687.

Leski, M. L. and Steward, O. (1996). Protein synthesis within dendrites: ionic and neurotransmitter modulation of synthesis of particular polypeptides characterized by gel electrophoresis. *Neurochem. Res.* **21**, 681-690.

Li, Y., Song, M. and Kiledjian, M. (2011). Differential utilization of decapping enzymes in mammalian mRNA decay pathways. *RNA* **17**, 419-428.

Lin, M. D., Jiao, X., Grima, D., Newbury, S. F., Kiledjian, M. and Chou, T. B. (2008). Drosophila processing bodies in oogenesis. *Dev. Biol.* **322**, 276-288.

Loschi, M., Leishman, C. C., Berardone, N. and Boccaccio, G. L. (2009). Dynein and kinesin regulate stress-granule and P-body dynamics. *J. Cell Sci.* **122**, 3973-3982.

Marin, P., Nastiuk, K. L., Daniel, N., Girault, J. A., Czernik, A. J., Glowinski, J., Nairn, A. C. and Prémont, J. (1997). Glutamate-dependent phosphorylation of elongation factor-2 and inhibition of protein synthesis in neurons. *J. Neurosci.* **17**, 3445-3454.

Miller, L. C., Blandford, V., McAdam, R., Sanchez-Carbente, M. R., Badeaux, F., DesGroseillers, L. and Sossin, W. S. (2009). Combinations of DEAD box proteins distinguish distinct types of RNA: protein complexes in neurons. *Mol. Cell. Neurosci.* **40**, 485-495.

Nagarajan, V. K., Jones, C. I., Newbury, S. F. and Green, P. J. (2013). XRN 5′→3′ exoribonucleases: structure, mechanisms and functions. *Biochim. Biophys. Acta* **1829**, 590-603.

Newbury, S. and Woollard, A. (2004). The 5′-3′ exoribonuclease xrn-1 is essential for ventral epithelial enclosure during C. elegans embryogenesis. *RNA* **10**, 59-65.

Park, E. and Maquat, L. E. (2013). Staufen-mediated mRNA decay. *Wiley Interdiscip Rev. RNA* **4**, 423-435.

Park, S., Park, J. M., Kim, S., Kim, J. A., Shepherd, J. D., Smith-Hicks, C. L., Chowdhury, S., Kaufmann, W., Kuhl, D., Ryazanov, A. G. et al. (2008). Elongation factor 2 and fragile X mental retardation protein control the dynamic translation of Arc/Arg3.1 essential for mGluR-LTD. *Neuron* **59**, 70-83.

Park, H. Y., Lim, H., Yoon, Y. J., Follenzi, A., Nwokafor, C., Lopez-Jones, M., Meng, X. and Singer, R. H. (2014). Visualization of dynamics of single endogenous mRNA labeled in live mouse. *Science* **343**, 422-424.

Pascual, M. L., Luchelli, L., Habif, M. and Boccaccio, G. L. (2012). Synaptic activity regulated mRNA-silencing foci for the fine tuning of local protein synthesis at the synapse. *Commun. Integr. Biol.* **5**, 388-392.

Pimentel, J. and Boccaccio, G. L. (2014). Translation and silencing in RNA granules: a tale of sand grains. *Front. Mol. Neurosci.* **7**, 68.

Pradhan, S. J., Nesler, K. R., Rosen, S. F., Kato, Y., Nakamura, A., Ramaswami, M. and Barbee, S. A. (2012). The conserved P body

component HPat/Pat1 negatively regulates synaptic terminal growth at the larval Drosophila neuromuscular junction. *J. Cell Sci.* **125**, 6105-6116.
Raab-Graham, K. F., Haddick, P. C., Jan, Y. N. and Jan, L. Y. (2006). Activity- and mTOR-dependent suppression of Kv1.1 channel mRNA translation in dendrites. *Science* **314**, 144-148.
Rymarquis, L. A., Souret, F. F. and Green, P. J. (2011). Evidence that XRN4, an Arabidopsis homolog of exoribonuclease XRN1, preferentially impacts transcripts with certain sequences or in particular functional categories. *RNA* **17**, 501-511.
Scheetz, A. J., Nairn, A. C. and Constantine-Paton, M. (2000). NMDA receptor-mediated control of protein synthesis at developing synapses. *Nat. Neurosci.* **3**, 211-216.
Schratt, G. (2009). microRNAs at the synapse. *Nat. Rev. Neurosci.* **10**, 842-849.
Sinturel, F., Bréchemier-Baey, D., Kiledjian, M., Condon, C. and Bénard, L. (2012). Activation of 5′-3′ exoribonuclease Xrn1 by cofactor Dcs1 is essential for mitochondrial function in yeast. *Proc. Natl. Acad. Sci. USA* **109**, 8264-8269.
Siwaszek, A., Ukleja, M. and Dziembowski, A. (2014). Proteins involved in the degradation of cytoplasmic mRNA in the major eukaryotic model systems. *RNA Biol.* **11**, 1122-1136.
Sosanya, N. M., Huang, P. P., Cacheaux, L. P., Chen, C. J., Nguyen, K., Perrone-Bizzozero, N. I. and Raab-Graham, K. F. (2013). Degradation of high affinity HuD targets releases Kv1.1 mRNA from miR-129 repression by mTORC1. *J. Cell Biol.* **202**, 53-69.
Souret, F. F., Kastenmayer, J. P. and Green, P. J. (2004). AtXRN4 degrades mRNA in Arabidopsis and its substrates include selected miRNA targets. *Mol. Cell* **15**, 173-183.
Sutton, M. A., Wall, N. R., Aakalu, G. N. and Schuman, E. M. (2004). Regulation of dendritic protein synthesis by miniature synaptic events. *Science* **304**, 1979-1983.
Sutton, M. A., Ito, H. T., Cressy, P., Kempf, C., Woo, J. C. and Schuman, E. M. (2006). Miniature neurotransmission stabilizes synaptic function via tonic suppression of local dendritic protein synthesis. *Cell* **125**, 785-799.
Sutton, M. A., Taylor, A. M., Ito, H. T., Pham, A. and Schuman, E. M. (2007). Postsynaptic decoding of neural activity: eEF2 as a biochemical sensor coupling miniature synaptic transmission to local protein synthesis. *Neuron* **55**, 648-661.
Tatavarty, V., Ifrim, M. F., Levin, M., Korza, G., Barbarese, E., Yu, J. and Carson, J. H. (2012). Single-molecule imaging of translational output from individual RNA granules in neurons. *Mol. Biol. Cell* **23**, 918-929.
Thomas, M. G., Martinez Tosar, L. J., Desbats, M. A., Leishman, C. C. and Boccaccio, G. L. (2009). Mammalian Staufen 1 is recruited to stress granules and impairs their assembly. *J. Cell Sci.* **122**, 563-573.
Thomas, M. G., Loschi, M., Desbats, M. A. and Boccaccio, G. L. (2011). RNA granules: the good, the bad and the ugly. *Cell. Signal.* **23**, 324-334.
Thomas, M. G., Luchelli, L., Pascual, M., Gottifredi, V. and Boccaccio, G. L. (2012). A monoclonal antibody against p53 cross-reacts with processing bodies. *PLoS ONE* **7**, e36447.
Thomas, M. G., Pascual, M. L., Maschi, D., Luchelli, L. and Boccaccio, G. L. (2014). Synaptic control of local translation: the plot thickens with new characters. *Cell. Mol. Life Sci.* **71**, 2219-2239.
Toretsky, J. A. and Wright, P. E. (2014). Assemblages: functional units formed by cellular phase separation. *J. Cell Biol.* **206**, 579-588.
Weiler, I. J. and Greenough, W. T. (1993). Metabotropic glutamate receptors trigger postsynaptic protein synthesis. *Proc. Natl. Acad. Sci. USA* **90**, 7168-7171.
Weiler, I. J., Spangler, C. C., Klintsova, A. Y., Grossman, A. W., Kim, S. H., Bertaina-Anglade, V., Khaliq, H., de Vries, F. E., Lambers, F. A., Hatia, F. et al. (2004). Fragile X mental retardation protein is necessary for neurotransmitter-activated protein translation at synapses. *Proc. Natl. Acad. Sci. USA* **101**, 17504-17509.
Yasuda, K., Zhang, H., Loiselle, D., Haystead, T., Macara, I. G. and Mili, S. (2013). The RNA-binding protein Fus directs translation of localized mRNAs in APC-RNP granules. *J. Cell Biol.* **203**, 737-746.
Zeitelhofer, M., Karra, D., Macchi, P., Tolino, M., Thomas, S., Schwarz, M., Kiebler, M. and Dahm, R. (2008). Dynamic interaction between P-bodies and transport ribonucleoprotein particles in dendrites of mature hippocampal neurons. *J. Neurosci.* **28**, 7555-7562.

Journal of Cell Science